# Charge disproportionation without charge transfer in the rare-earth nickelates as a possible mechanism for the metal-insulator transition

Steve Johnston, 1,2 Anamitra Mukherjee, 1 Ilya Elfimov, 1,2 Mona Berciu, 1,2 and George A. Sawatzky 1,2,3

<sup>1</sup>Department of Physics and Astronomy, University of British Columbia, Vancouver, British Columbia, Canada V6T 1Z1

<sup>2</sup>Quantum Matter Institute, University of British Columbia, Vancouver, British Columbia, Canada V6T 1Z4

<sup>3</sup>Department of Chemistry, University of British Columbia, Vancouver, British Columbia, Canada V6T 1Z1

(Dated: August 4, 2018)

We study a model for the metal-insulator (MI) transition in the rare-earth nickelates RNiO<sub>3</sub>, based upon a negative charge transfer energy and coupling to a rock-salt like lattice distortion of the NiO<sub>6</sub> octahedra. Using exact diagonalization and the Hartree-Fock approximation we demonstrate that electrons couple strongly to these distortions. For small distortions the system is metallic, with ground state of predominantly  $d^8\underline{L}$  character, where  $\underline{L}$  denotes a ligand hole. For sufficiently large distortions  $(\delta d_{\text{Ni-O}} \sim 0.05-0.10 \mathring{A})$ , however, a gap opens at the Fermi energy as the system enters a periodically distorted state alternating along the three crystallographic axes, with  $(d^8\underline{L}^2)_{S=0}(d^8)_{S=1}$  character, where S is the total spin. Thus the MI transition may be viewed as being driven by an internal volume "collapse" where the NiO<sub>6</sub> octahedra with two ligand holes shrink around their central Ni, while the remaining octahedra expand accordingly, resulting in the (1/2,1/2,1/2) superstructure observed in x-ray diffraction in the insulating phase. This insulating state is an example of a new type of charge ordering achieved without any actual movement of the charge.

PACS numbers: 71.30.+h, 71.38.-k, 72.80.Ga

The perovskite rare-earth nickelates RNiO<sub>3</sub> undergo a first order metal-insulator (MI) transition at a transition temperature T<sub>MI</sub> that can be tuned via pressure, strain, or variations in the radius of the R ion  $(R \neq La)$  [1, 2]. These systems have received considerable attention for over two decades as a means for studying MI transitions; this has intensified in recent years due to proposals for application in heterostructures [3–5]. However, despite this long history, the precise mechanism for the MI transition is still not fully understood and a number of competing proposals have been made. These include a closing of the charge transfer gap [2], Jahn-Teller polarons [6], the formation of long-range magnetic order (if R = Nd, Pr) [7, 8], charge ordering on the Ni sites, often referred to as charge disproportionation (CD) [1, 9–15], or more complex charge ordering distributed over the Ni and O sites, with the possible involvement of the lattice [16–18].

The leading interpretation for the MI transition is CD between the Ni sites. Several structural changes are concomitant with the MI transition, such as subtle changes in the Ni-O-Ni bond angle and changes in the Ni-O bond lengths resulting in a lowering of the crystal symmetry from an orthorhombic Pbnm to a monoclinic  $P2_1/n$ spacegroup [1, 9, 12, 13, 19]. This forms two inequivalent Ni sites, where the NiO<sub>6</sub> octahedra contract and expand, respectively, about alternating sites along the three crystallographic axes. Formal valence counting suggests that the  $Ni^{3+}$  ions are in a  $3d^{7}$  valence state and the inequivalent Ni sites are interpreted as a  $3d^73d^7 \rightarrow 3d^{(7-\delta)}3d^{(7+\delta)}$ CD below  $T_{\rm MI}$  [9–11, 14]. This CD is thought to drive the MI transition, however it is not clear whether the electron-lattice or the on-site electron-electron interactions drive the charge ordering.  $T_{\rm MI}$  exhibits a large  $^{16}{\rm O}$ 

-  $^{18}{\rm O}$  isotope effect [6], confirming that the lattice and electronic degrees of freedom are strongly coupled, and the latter could be driven by the former. A recent proposal views the lattice distortion as a secondary effect to a magnetic ordering [7, 8], however this picture is difficult to apply to systems with  $T_{\rm N} < T_{\rm MI}$ , which is the case across much of the phase diagram [1].

The CD scenario assumes that Ni  $3d^7$  is the appropriate starting point for describing the nickelates, but a few open issues remain. In the (nearly) cubic structure, the Ni  $3d^7$   $(t_{2q}^6 e_q^4)$  ion has two degenerate  $e_q$  orbitals which the system will prefer to lift via a coherent Jahn-Teller effect or via CD between neighbouring Ni sites. There is no sign of a JT distortion [6] like the orbital ordering in manganites [20], which also have a singly occupied degenerate  $e_q$  orbital. On the other hand, CD should be suppressed by the large Hubbard U, however it can be stabilized by a sizeable Hunds coupling if the system is close to the itinerant limit [21]. This is likely the case in the rareearth nickelates, which have been classified as small or negative charge transfer systems [16–18, 22–28]. In such conditions, however, it becomes energetically favourable to transfer a hole from Ni to ligand O sites [29], and Ni  $3d^7$  is no longer the appropriate starting point. Rather, one should begin with a Ni  $d^8$ L state in the atomic limit, which is equivalent to taking a negative charge transfer energy before allowing for hybridization between the Ni and O atoms. In this picture, the ground state would have, on average, one ligand hole per NiO<sub>3</sub> unit.

Ligand holes can couple strongly to the bondstretching O vibrations which modulate the hybridization between the TM and O sites [6, 30]. Thus, the carriers in nickelates (which are primarily O ligand holes

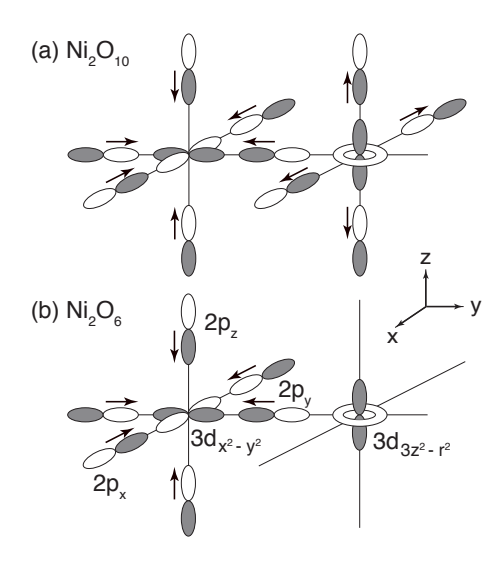


FIG. 1: (a)  $Ni_2O_{10}$  quasi-1D cluster with periodic boundary conditions along the y-axis, studied with ED. Both Ni 3d eg orbitals are included at each Ni site, but only one orbital per Ni is depicted here to establish our phase convention. (b)  $Ni_2O_6$  unit cell used for our 3D calculations using HFA. The arrows in both panels indicate the displacement pattern for the rock-salt-like oxygen distortion.

in our picture) can couple strongly to the rock-salt-like lattice distortions. In this Letter we examine this scenario as a means for explaining the MI transition. Using exact diagonalization (ED) and Hartree-Fock (HF) calculations [31, 32] we confirm that a strong electron-lattice coupling drives the system through a MI transition for sufficiently large and experimentally relevant lattice distortions ( $\delta d_{\rm Ni-O} \sim 0.05\text{-}0.1 \text{Å}$ ). In the insulating phase we find a novel charge ordering which can be viewed as a  $(d^8\underline{L})_i(d^8\underline{L})_j \to (d^8\underline{L}^2)_{S=0}(d^8)_{S=1}$  type, where S is the total spin. In this picture, the MI transition results from a partial volume collapse of NiO<sub>6</sub> octahedra with two ligand holes around their central Ni, while the other octahedra expand accordingly with little net effect on the total volume, as observed experimentally [1]. However, since each O is shared by a collapsed and an expanded octahedron, in fact all octahedra have the same average hole concentration. The difference is that the two ligand holes acquire the symmetry of the  $e_q$  orbitals of the Ni in the collapsed  $d^{8}\underline{L}^{2}$  octahedron, which therefore becomes formally equivalent to a  $3d^6$  state that is effectively no longer JT active, and attains a spin of zero. Thus, as far as symmetry and spin are concerned, this new charge state appears as a fully CD state, but one achieved without actual movement of charge. We note that a similar charge/spin distribution was proposed in Refs. 17, 18, but as being driven by very different mechanisms.

We investigate quasi-one-dimensional (1D) and three-dimensional (3D) clusters/unit cells. In each case, the orbital basis includes both  $3d\ e_g$  orbitals at each Ni site

and the  $2p_{\sigma}$  orbital at each O site, as shown in Fig. 1. The microscopic Hamiltonian for the electronic degrees of freedom is  $H=H_0+H_{\rm int}$ , where

$$H_0 = \sum_{i,\alpha} \epsilon_{\alpha} d_{i,\alpha,\sigma}^{\dagger} d_{i,\alpha,\sigma} + \sum_{i,j,\alpha,\beta,\sigma} t_{ij}^{\alpha\beta} d_{i,\alpha,\sigma}^{\dagger} d_{j,\beta,\sigma}$$

contains the non-interacting on-site and near-neighbor hopping terms, and

$$H_{\text{int}} = \sum_{i,\alpha,\sigma\neq\sigma'} \frac{U}{2} n_{i,\alpha,\sigma} n_{i,\alpha,\sigma'} + \sum_{i,\alpha\neq\alpha',\sigma,\sigma'} \frac{U'}{2} n_{i,\alpha,\sigma} n_{i,\alpha',\sigma'}$$

$$+ \sum_{i,\alpha,\alpha',\sigma,\sigma'} \frac{J}{2} d^{\dagger}_{i,\alpha,\sigma} d^{\dagger}_{i,\alpha',\sigma'} d_{i,\alpha,\sigma'} d_{i,\alpha',\sigma}$$

$$+ \sum_{i,\alpha\neq\alpha',\sigma\neq\sigma'} \frac{J'}{2} d^{\dagger}_{i,\alpha,\sigma} d^{\dagger}_{i,\alpha,\sigma'} d_{i,\alpha',\sigma'} d_{i,\alpha',\sigma}$$

contains the on-site Coulomb interactions with  $n_{i,\alpha,\sigma}=d_{i,\alpha,\sigma}^{\dagger}d_{i,\alpha,\sigma}$ , where  $d_{i,\alpha,\sigma}^{\dagger}$  creates a spin- $\sigma$  electron in one of the two  $e_g$  orbitals if i is a Ni site, or the  $2p_{\sigma}$  orbital if i is an O site. In eV units we set  $U_d=7$ ,  $J_d=J_d'=0.9$ ,  $U_d'=U_d-2J_d$ ,  $U_p=5$ ,  $\epsilon_d=0$ ,  $\epsilon_p=2.25$ ,  $(pd\sigma)=-1.8$ ,  $(pp\sigma)=0.6$ ,  $(pd\pi)=-(pd\sigma)/2$ , and  $(pp\pi)=-(pp\sigma)/4$ . For these parameters the ground state of an isolated NiO<sub>6</sub> octahedron is  $|\Psi\rangle=\alpha|d^7\rangle+\beta|d^8\underline{L}\rangle+\gamma|d^9\underline{L}^2\rangle$  with  $\beta^2\approx0.56$ , i.e. the system is in the negative charge transfer regime and the ground state has predominantly  $d^8\underline{L}$  character, in agreement with experiment [22–25].

The lattice degrees of freedom are treated in the adiabatic limit as frozen lattice displacements [33], i.e. all O atoms are displaced equally along the rock-salk displacement pattern indicated by arrows in Fig. 1. The electronlattice coupling is introduced by rescaling the Ni-O and O-O transfer integrals. Specifically, we take  $t_{pd} = t_{pd}^0 (1 +$  $\delta d_{\text{Ni-O}}/d_{\text{Ni-O}})^{-3}$  and  $t_{pp} = t_{pp}^0 (1 + \delta d_{\text{O-O}}/d_{\text{O-O}})^{-4}$  [18, 34], where  $\delta d$  is the change in the appropriate bond length with respect to  $d_{\text{Ni-O}} = d_{\text{O-O}}/\sqrt{2} = 1.95 \text{ Å in}$ the undistorted structure. The lattice potential energy adds an overall quadratic term to the total energy, while the lattice kinetic energy is neglected. From now on all displacements are reported in terms of  $\delta d_{N_{i-O}}$ , and we drop its subscript for brevity. We note that we have also tested the other possible displacement patterns for the O atoms, however the static rock-salt-like pattern discussed here produces the lowest energy [35].

We first consider two neighbouring NiO<sub>6</sub> octahedra in the quasi-1D cluster of Fig. 1(a) with three holes/Ni; this can be solved exactly using ED. Fig. 2(a) shows the electronic contribution to its ground state energy,  $E_{el}$ , in the  $(3 \uparrow 3 \downarrow)$  and  $(4 \uparrow 2 \downarrow)$  sectors as a function of  $\delta d$ . Figs. 2(b), (c) show average hole occupations at Ni and O sites for the compressed (solid symbols) and expanded (open symbols) NiO<sub>6</sub> octahedra. Both sectors exhibit a sizable decrease in the electronic energy with increasing displacement, indicating a rather strong electron-lattice

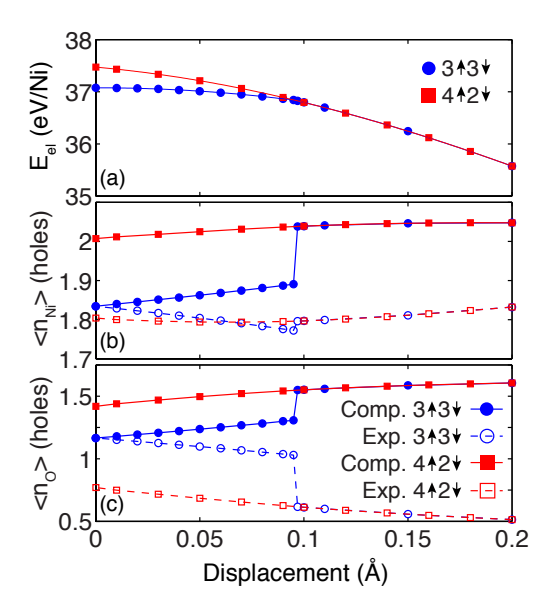


FIG. 2: (color online) A summary of ED results for the  $\text{Ni}_2\text{O}_{10}$  cluster. (a) Electronic contribution to the ground state energy in the  $(3 \uparrow 3 \downarrow)$  (blue  $\bigcirc$ ) and  $(4 \uparrow 2 \downarrow)$  (red  $\square$ ) sectors as a function of the static O displacement. (b), (c) Average hole occupancy at Ni and O sites, respectively. Sites on the left (right) side of the  $\text{Ni}_2\text{O}_{10}$  cluster correspond to the compressed (expanded)  $\text{NiO}_6$  octahedron for  $\delta d > 0$  (see Fig. 1), and are represented by the solid (open) symbols.

coupling. The  $(3 \uparrow 3 \downarrow)$  sector exhibits a kink in  $E_{el}$  for a critical displacement  $\delta d_c \sim 0.097$  Å, indicative of a level crossing and a change in the ground state wave function as a function of displacement.

For  $\delta d = 0$  the ground state has a total spin  $S_{\text{tot}} = 0$ with majority  $(d^8\underline{L})(d^8\underline{L})$  character, as expected for a negative value of  $\Delta$ . This state persists as the ground state for small  $\delta d < \delta d_c$ , however a small redistribution of charge occurs between the two octahedra due to the increased delocalization on the compressed side. For  $\delta d > \delta d_c$  a different ground state is obtained with  $S_{\rm tot}=1$  and  $m_z=0$ . (In the  $4\uparrow 2\downarrow$  sector the  $S_{\rm tot}=1$ ,  $m_z = \pm 1$  counterparts of this state form the degenerate ground state for all values of  $\delta d$ .) The new state possesses an interesting redistribution of charge. Both Ni ions are in a  $d^8$  spin triplet state while the L hole of the expanded octahedron transfers to the compressed side, where the two L<sup>2</sup> holes lock in a triplet pair due to the finite value of  $U_p$  [36]. The  $\underline{L}^2$  spin couples antiferromagnetically to the central Ni spin, leaving the system in a  $(d^8L^2)_{S=0}(d^8)_{S=1}$ state. Thus, for sufficiently large rock-salt-like displacements, the ligand hole of the expanded octahedron can re-associate with a neighbouring NiO<sub>6</sub> octahedron leaving a lone S=1 spin on alternating Ni sites and a small  $CD \sim 0.1$  between the two inequivalent Ni sites. We note that the critical value  $\delta d_c$  obtained here is slightly larger than the typical changes in bond length  $\sim 0.052$  - 0.092  $\mathring{A}$  reported in the insulating phase [9, 10, 14].

Below the MI transition a rock-salt distortion exists in the nickelates and a similar re-association of the ligand holes may occur in the 3D system as well. However, while for the Ni<sub>2</sub>O<sub>10</sub> cluster we can assign the O sites to unique octahedra, in the bulk 3D system this is not possible since each O is shared by an expanded and a contracted octahedron. The  $\underline{L}^2$  triplet pairs assigned to the collapsed NiO<sub>6</sub> octahedra are formed between the ligand hole of the compressed NiO<sub>3</sub> unit and a second hole provided by the neighbouring expanded NiO<sub>3</sub> units. From a charge counting perspective, each of the NiO<sub>3</sub> units still has one ligand hole and hence the system appears to have dominant  $d^{8}\underline{L}$  character. What is changed is not the ligand holes' average distribution, but the phases in their wavefunction which now acquire the symmetry of the two  $e_q$ orbitals of the Ni in the collapsed octahedron. The basic effect is similar to the Zhang-Rice singlet scenario in the cuprates where the ligand hole selects the relative phases of the four oxygen orbitals so as to maximally hybridize with one of the two Cu ions bridged by the oxygen.

We stress that this is a very different form of charge ordering than the commonly discussed CD; it should be thought of as a novel charge ordering without a significant movement of charge.

We now turn to a quantitative analysis of the 3D case, and examine an extended lattice that cannot be handled using ED. We therefore implement an unbiased HFA [32] (see the supplementary material for details [35]). One might doubt the validity of the HFA given the strong correlations on the Ni sites, however the large bandwidth O 2p bands overlap with the Ni states because of the negative charge transfer energy. This reduces significantly the effects of correlations, explaining why a number of studies have had success with mean-field approaches [16, 18, 22]. To verify that the HFA captures the physics of our model we compare its predictions to ED results for a  $Ni_2O_6$  cluster with periodic boundary conditions, see Fig. 1(b).  $E_{el}$ results are shown in Fig. 3(a). Not surprisingly, the HFA has higher ground state energies ( $\sim 1 \text{ eV}$ ), but it correctly reproduces the displacement dependence and the average hole occupations [35]. This gives us confidence that HFA is reasonably accurate for this Hamiltonian.

Scaling to the extended lattice, Figs. 3(b)-(e) show HF results obtained for a 3D system with  $0.5 \times 40^3$  momentum points in the Brillouin zone. The electronic component of the ground state energy,  $E_{el}$ , (Fig. 3b) essentially mirrors the ED results, exhibiting large variation with lattice displacement. This confirms the strong electron-lattice coupling even within the HFA. The hole occupancies n (Fig. 3c) and Ni magnetization  $m_z$  (Fig. 3d) also follow the expectations gained from the Ni<sub>2</sub>O<sub>10</sub> cluster. For small  $\delta d$  the total occupancies of the two Ni sites start to separate until  $\delta d \sim 0.03$  -  $\sim 0.04$  Å, when they gradually level off. At the same time the magnetizations of the two  $e_g$  orbitals in the compressed octahedron fall to zero as each  $e_g$  orbital is occupied by half an electron of each

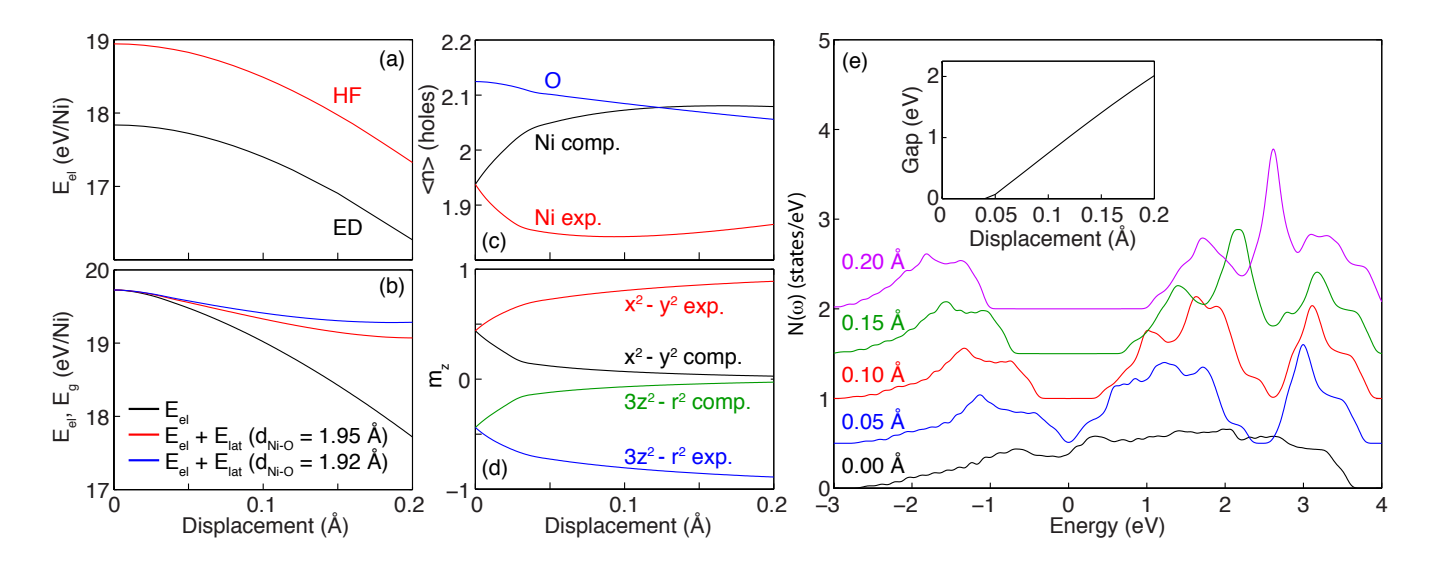


FIG. 3: (color online) (a) A comparison of the dependence of the HFA (red/light) and ED (black/dark) ground state energies of the Ni<sub>2</sub>O<sub>6</sub> cluster as a function of the oxygen displacement. (b)-(e) HFA results for the 3D lattice with  $80 \times 80 \times 80/2$  momentum points in the Brillouin zone: (b) ground state electronic energy, (c) average hole occupation of the oxygen (blue) sites and the compressed/expanded Ni sites (black/red), (d) magnetization  $m_z = (n_{\uparrow} - n_{\downarrow})$  of the Ni orbitals, (e) single particle density of states for several oxygen displacements. The spectrum has been lifetime broadened with a Lorentzian (HFHM = 25 meV). Another band of states is located below 3 eV (not shown). The inset shows the gap as a function of displacement.

spin species, on average. Similarly, the magnetization of each  $e_g$  orbital in the expanded octahedron rapidly grows to nearly one but with opposite alignments. The magnetization of the O sites (not shown) is nearly zero for all values of  $\delta d$ . Although the HFA cannot reproduce the triplet correlations of the exact cluster solution, these results mimick the  $(d^8\underline{L}^2)_{S=0}(d^8)_{S=1}$  ground state observed in the small cluster and therefore confirm our picture of the novel charge ordering.

Next, we calculate the single particle density of states  $N(\omega)$  as a function of  $\delta d$ , see Fig. 3(e). For  $\delta d=0$ ,  $N(\omega)$  has finite weight at the Fermi energy  $\omega=0$ , consistent with metallic behavior in a negative charge transfer system.  $N(\omega=0)$  is suppressed for increasing  $\delta d$  until  $\delta d\approx 0.05$  Å, where a gap that increases linearly with  $\delta d$  opens up (inset, Fig. 3(e)). We stress that this gap is the result of the alternating expanded and contracted octahedra rather than the formation of the  $(S=0)_i(S=1)_j$  magnetic structure, because similar sized gaps are observed even when we restrict the HFA by enforcing identical Ni sites. We conclude that the gap opens due to the electron-lattice interaction and rock-salt lattice distortions, consistent with the MI transition observed in these materials.

We complete our discussion with an estimate for the energy cost of the octahedral distortions, based on density functional theory (DFT) within the generalized gradient approximation (GGA)[37, 38]. The total energy was calculated for the cubic LaNiO<sub>3</sub> structure with lattice constants of 3.9  $\mathring{A}$  and 3.84  $\mathring{A}$ , the latter being the DFT prediction [39]. In both cases we find the change

in total energy to increase like  $(\delta d)^2$ . We use this change in total energy as a very rough estimate of the potential energy of the lattice distortion [40]. Fig. 3(b) shows the total energy obtained by adding this contribution to  $E_{el}$  obtained from the HFA. The total energy possesses a deep minimum for  $\delta d \sim 0.17-0.2$  Å. This is a factor of two larger than the experimental value, but reasonable given the crudeness of our estimate for the lattice contribution. Note that a strong isotope effect is obviously consistent with this model of the MI transition.

In summary, we have examined the consequences of the interplay between a negative charge transfer energy and the electron-lattice coupling in RNiO<sub>3</sub>, starting from a  $d^8\underline{L}$  atomic configuration. Our results demonstrate that in this parameter regime a strong electron-lattice interaction arises and that it drives a MI transition. In this picture, the nickelates undergo a new type of effective CD achieved without any significant movement of charge between neighbouring NiO<sub>6</sub> octahedra. In order to verify whether such a picture extends across the whole family of nickelates, systematic studies capable of incorporating more accurately the lattice potential are required.

Acknowledgements - We thank M. W. Haverkort for useful discussions. This work was supported by NSERC, CIfAR, and the Max Planck - UBC Centre for Quantum Materials.

- M. L. Medarde, J. Phys.: Condens. Matter 9, 1679 (1997).
- [2] J. B. Torrance, P. Lacorre, A. I. Nazzal, E. J. Ansaldo, and Ch. Niedermayer, Phys. Rev. B 45, 8209(R) (1992).
- [3] J. Chaloupka and Giniyat Khaliullin, Phys. Rev. Lett. 100, 016404 (2008).
- [4] P. Hansmann, X. Yang, A. Toschi, G. Khaliullin, O. K. Andersen, and K. Held, Phys. Rev. Lett. 103, 016401 (2009).
- [5] J Liu, S. Okamoto, M. van Veenendaal, M. Kareev, B. Gray, P. Ryan, J. W. Freeland, and J. Chakhalian, Phys. Rev. B 83, 161102(R) (2011).
- [6] M. Medarde, P. Lacorre, K. Conder, F. Fauth, and A. Furrer, Phys. Rev. Lett. 80, 2397 (1998).
- [7] S. B. Lee, R. Chen, and L. Balents, Phys. Rev. B 84, 165119 (2011).
- [8] S. B. Lee, R. Chen, and L. Balents, Phys. Rev. Lett. 106, 016405 (2011).
- [9] J. A. Alonso, M. J. Martínez-Lope, I. A. Presniakov, A. V. Sobolev, V. S. Rusakov, A. M. Gapochka, G. Demazeau, and M. T. Fernández-Díaz, Phys. Rev. B 87, 184111 (2013).
- [10] M. Medarde, M. T. Fernández-Díaz, and Ph. Lacorre, Phys. Rev. B 78, 212101 (2008).
- [11] M. Medarde, C. Dallera, M. Grioni, B. Delley, F. Vernay, J. Mesot, M. Sikora, J. A. Alonso, and M. J. Martínez-Lope, Phys. Rev. B 80, 245105 (2009).
- [12] J. A. Alonso, M. J. Martínez-Lope, M. T. Casais, J. L. García-Muñoz, and M. T. Fernández-Díaz, Phys. Rev. B 61, 1756 (2000)
- [13] J. A. Alonso, M. J. Martínez-Lope, M. T. Casais, J. L. García-Muñoz, M. T. Fernández-Díaz, and M. A. G. Aranda, Phys. Rev. B 64, 094102 (2001).
- [14] J. L. García-Muñoz, M. A. G. Aranda, J. A. Alonso, and M. J. Martínez-Lope, Phys. Rev. B 79, 134432 (2009).
- [15] J. A. Alonso, J. L. Garcia-Muñoz, M. T. Fernández-Díaz, M. A. G. Aranda, M. J. Martinez-Lope, and M. T. Casais, Phys. Rev. Lett. 82, 3871 (1999).
- [16] T. Mizokawa, D. I. Khomskii, and G. A. Sawatzky, Phys. Rev. B 61, 11263 (2000).
- [17] H. Park, A. J. Millis, and C. A. Marianetti, Phys. Rev. Lett. 109, 156402 (2012).
- [18] B. Lau and A. J. Millis, Phys. Rev. Lett. 110, 126404 (2013).
- [19] C. Piamonteze, H. C. N. Tolentino, A. Y. Ramos, N. E. Massa, J. A. Alonso, M. J. Martínez-Lope, and M. T. Casais, Phys. Rev. B 71, 012104 (2005).
- [20] P. Norby, İ.G.Krogh Andersen, E.Krogh Andersen, and N.H. Andersen, J. Solid State Chem. 119, 192 (1995).

- [21] I. I. Mazin, D. I. Khomskii, R. Lengsdorf, J. A. Alonso, W. G. Marshall, R. M. Ibberson, A. Podlesnyak, M. J. Martínez-Lope, and M. M. Abd-Elmeguid, Phys. Rev. Lett. 98, 176406 (2007).
- [22] T. Mizokawa, A. Fujimori, T. Arima, Y. Tokura, N. Mori, and J. Akimitsu, Phys. Rev. B 52, 13865 (1995).
- [23] Y. Bodenthin, U. Staub, C. Piamonteze, M. García-Fernández, M. J. Martínez-Lope, and J. A. Alonso, J. Phys.: Condens. Matter 23 036002 (2011).
- [24] M. Abbate, G. Zampieri, F. Prado, A. Caneiro, J. M. Gonzalez-Calbet, and M. Vallet-Regi, Phys. Rev. B 65, 155101 (2002).
- [25] K. Horiba, R. Eguchi, M. Taguchi, A. Chainani, A. Kikkawa, Y. Senba, H. Ohashi, and S. Shin, Phys. Rev. B 76, 155104 (2007).
- [26] Myung Joon Han and Michel van Veenendaal, Phys. Rev. B 85, 195102 (2012).
- [27] A. Blanca-Romero and R. Pentcheva, Phys. Rev. B 84, 195450 (2011).
- [28] V. I. Anisimov, D. Bukhvalov, and T. M. Rice, Phys. Rev. B 59, 7901 (1999).
- [29] J. Zaanen, G. A. Sawatzky, and J. W. Allen, Phys. Rev. Lett. 55, 418 (1985).
- [30] O. Rösch and O. Gunnarsson, Phys. Rev. B 70, 224518 (2004).
- [31] C.-C. Chen, B. Moritz, C. J. Jia, S. Johnston, A. P. Sorini, L.-Q. Lee, K. Ko, and T. P. Devereaux, Computer Physics Communications 182, 106 (2011).
- [32] J.-P. Blaizot and G. Ripka, Quantum Theory of Finite Systems. The MIT Press (1986).
- [33] This can also be viewed as a variational calculation where the quantum phonons at each O site are in the coherent state consistent with its displacement.
- [34] W.A. Harrison, Elementary Electronic Structure (World Scientific, Singapore, 1999).
- [35] See online supplementary material.
- [36] I. S. Elfimov, S. Yunoki, and G. A. Sawatzky, Phys. Rev. Lett. 89, 216403 (2002).
- [37] J. P. Perdew, K. Burke, and M. Ernzerhof, Phys. Rev. Lett. 77, 3865 (1996).
- [38] P. Blaha, et al., WIEN2k: An Augmented Plane Wave plus Local Orbitals Program for Calculating Crystal Properties (TU Wien, 2001 (ISBN 3-9501031-1-2)).
- [39] DFT calculations were performed using code WIEN2K[38] and FCC  $(Fm\bar{3}m)$  supercell with 2 formula units. Self-consistency was obtained with 1000 k points in the reduced Brillouin zone.
- [40] This should be regarded as a very rough estimate as the change in covalency due to the lattice deformation is doubly counted in this approach.

## Charge disproportionation without charge transfer in the rare-earth nickelates as a possible mechanism for the metal-insulator transition - supplementary material

Steve Johnston, <sup>1,2</sup> Anamitra Mukherjee, <sup>1</sup> Ilya Elfimov, <sup>1,2</sup> Mona Berciu, <sup>1,2</sup> and George A. Sawatzky <sup>1,2,3</sup>

PACS numbers: 71.30.+h, 71.38.-k, 72.80.Ga

#### PHONON DISPLACEMENT PATTERN

In order to verify that the rock-salt-like distortion pattern assumed in the main text is energetically favored we performed a series of ED calculations for the  $\mathrm{Ni_2O_{10}}$  cluster. In each case we allowed the ten O atoms to be displaced by  $\delta d=\pm0.1$  Å along the Ni-O bond direction. ED calculations for the ground state energy were then carried out for the  $2^{10}$  possible configurations. The lowest energies were obtained for the two displacement patterns corresponding to a contraction/expansion or expansion/contraction of the O octahedra about the two Ni sites as considered in the article.

### HARTREE-FOCK CALCULATIONS

We performed unbiased Hartree-Fock calculations for the model Hamiltonian given in the main text. Our treatment follows that of Ref. 1, which we summarize here for completeness. We work in momentum space where the microscopic Hamiltonian can be rewritten in the form

$$H = \sum_{\mathbf{k},\alpha,\beta,\sigma} T_{\alpha,\beta}(\mathbf{k}) d^{\dagger}_{\mathbf{k},\alpha,\sigma} d_{\mathbf{k},\beta,\sigma} + \sum_{\alpha,\alpha',\beta,\beta',\sigma,\sigma'} \sum_{\mathbf{k},\mathbf{k'},\mathbf{q}} U^{\sigma,\sigma'}_{\alpha,\alpha',\beta,\beta'}(\mathbf{q}) d^{\dagger}_{\mathbf{k},\alpha,\sigma} d^{\dagger}_{\mathbf{k'},\alpha',\sigma'} d_{\mathbf{k'}-\mathbf{q},\beta',\sigma'} d_{\mathbf{k}+\mathbf{q},\beta,\sigma}.$$
(S1)

where the interaction on a Ni site is given by

$$U_{\alpha,\alpha',\beta,\beta'}^{\sigma\sigma'} = \frac{U}{2} \delta_{-\sigma,\sigma'} \delta_{\alpha,\alpha'} \delta_{\alpha\beta} \delta_{\alpha\beta'} + \frac{U'}{2} (1 - \delta_{\alpha\alpha'}) \delta_{\alpha\beta} \delta_{\alpha'\beta'}$$

$$+ \frac{J}{2} (1 - \delta_{\alpha\alpha'}) \delta_{\alpha\beta'} \delta_{\alpha'\beta} + \frac{J'}{2} \delta_{\alpha\alpha'} \delta_{\beta\beta'} (1 - \delta_{\sigma\sigma'}) (1 - \delta_{\alpha\beta}).$$
(S2)

The interaction on an O site is like the first term with U replaced by  $U_n$ .

Our aim is to now construct a HF Hamiltonian of the form

$$H_{\rm HF} = \sum_{n,\mathbf{k}} E_n(\mathbf{k}) \gamma_{n,\mathbf{k},\sigma}^{\dagger} \gamma_{n,\mathbf{k},\sigma}, \tag{S3}$$

where n is a band index and  $\mathbf{k}$  is the electron momentum restricted to the first Brillouin zone. We begin by expanding the HF operators in terms of the original basis set  $\gamma_{\mathbf{k},n,\sigma} = \sum_{\alpha} c_{n,\alpha}(\mathbf{k}) d_{\mathbf{k},\alpha,\sigma}$ , and then obtain the HF matrix equation for the expansion coefficients  $\sum_{\alpha} M_{\alpha\beta}(\mathbf{k}) c_{\alpha}(\mathbf{k}) = E_n(\mathbf{k}) c_{\alpha}(\mathbf{k})$ , which is solved self-consistently. The matrix  $M_{\alpha\beta}(\mathbf{k})$  results from the equation:

$$\langle \left\{ [\gamma_{n,\mathbf{k},\sigma}, H], d_{\mathbf{k},\alpha',\sigma'}^{\dagger} \right\} \rangle = \left\{ E_n(\mathbf{k}) \gamma_{n,\mathbf{k},\sigma}, d_{\mathbf{k},\alpha',\sigma'}^{\dagger} \right\}. \tag{S4}$$

For a quadratic Hamiltonian the left-hand side result of the commutators/anticommutators is a c-number and no average would be needed. For a quartic Hamiltonian that side contains operators which are replaced with their HF values. This method leads to the true unbiased HF solution (i.e., the Slater determinant that minimizes the total energy, see [1]).

After lengthy but straightforward algebra we find:

$$M_{\alpha\beta}(\mathbf{k}) = T_{\alpha,\beta}(\mathbf{k}) + \frac{1}{2} \sum_{\mathbf{q},\alpha',\beta',\sigma'} \left[ U_{\beta,\alpha',\alpha,\beta'}^{\sigma\sigma'} + U_{\alpha',\beta,\beta',\alpha}^{\sigma'\sigma} \right] \langle d_{\mathbf{q},\alpha',\sigma'}^{\dagger} d_{\mathbf{q},\beta',\sigma'} \rangle$$

$$- \frac{1}{2} \sum_{\mathbf{q},\alpha',\beta'} \left[ U_{\alpha',\beta,\alpha,\beta'}^{\sigma\sigma} + U_{\beta,\alpha',\beta',\alpha}^{\sigma\sigma} \right] \langle d_{\mathbf{q},\alpha',\sigma}^{\dagger} d_{\mathbf{q},\beta',\sigma} \rangle$$
(S5)

<sup>&</sup>lt;sup>1</sup>Department of Physics and Astronomy, University of British Columbia, Vancouver, British Columbia, Canada V6T 1Z1

<sup>2</sup>Quantum Matter Institute, University of British Columbia, Vancouver, British Columbia, Canada V6T 1Z4

<sup>3</sup>Department of Chemistry, University of British Columbia, Vancouver, British Columbia, Canada V6T 1Z1

(Dated: August 4, 2018)

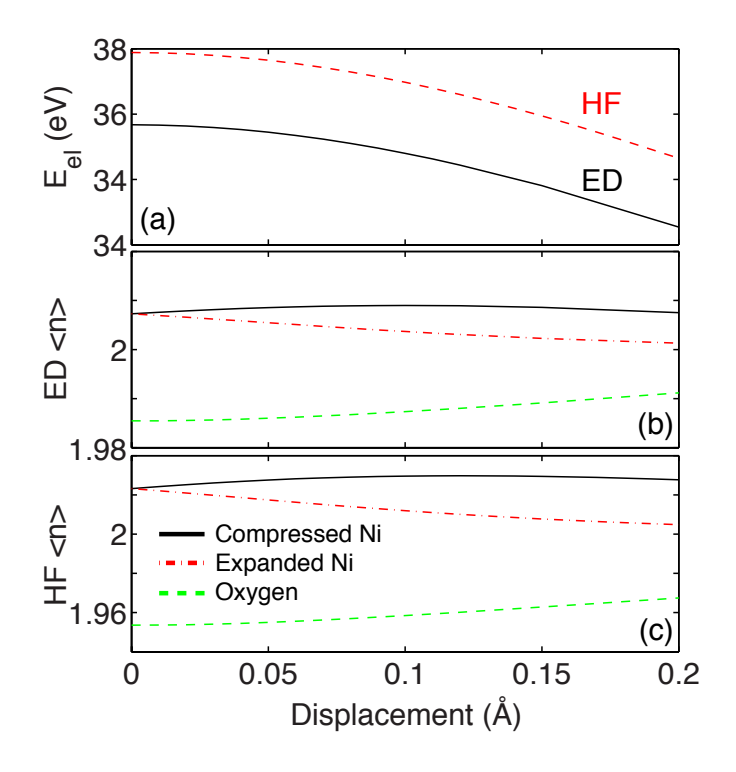


FIG. S1: (color online) (a) The ground state energy per Ni atom of the  $Ni_2O_6$  cluster with periodic boundary conditions. HF (red/dashed) and ED (black/solid) results are shown. (b) The total hole occupancy of the compressed Ni (black/solid), expanded Ni (red/dash-dot), and O (green/dashed) sites as obtained from ED. (c) As panel (b) but obtained within the HF treatment.

where the average  $\langle \rangle$  defines the self-consistent HF fields, which are found iterationally. It should be noted that the dependence on the static lattice displacement is introduced through the kinetic term  $T_{\alpha,\beta}(\mathbf{k})$ , see main text.

### COMPARISON WITH EXACT DIAGONALIZATION

Here we compare the results of the HFA with those obtained from exact diagonalization for the  $Ni_2O_6$  cluster where periodic boundary conditions have been assumed such that only the  $\mathbf{k}=0$  momentum point is included. Fig. S1a shows a comparison of the ground state energy (electronic component only), identical to the results shown in Fig. 3(a) of the main text. In general the HF treatment overestimates the exact answer by  $\sim 1$  eV, however the overall dependence on displacement is well reproduced. This general behavior also holds for the total hole occupancies, shown in Fig. S1b and S1c for the exact and HF solutions, respectively. This comparison gives us confidence that the HF method can describe the physics of the nickelates for our choice in parameters.

[1] J.-P. Blaizot and G. Ripka, Quantum Theory of Finite Systems. The MIT Press (1986).